INTRINSIC-CARRIER THERMAL RUNAWAY IN SILICON MICROCANTILEVERS

B. W. Chui, M. Asheghi, Y. S. Ju, K. E. Goodson, and T. W. Kenny
Stanford University, Stanford, California, USA

H. J. Mamin
IBM Almaden Research Center, San Jose, California, USA

A variety of micromachined sensors and actuators use coupled electrical and thermal transport in doped silicon bridges and cantilevers. One example is thermomechanical data storage cantilevers, in which Joule heating and atomic-scale forces yield indentations in an organic substrate. The thermal isolation of these structures augments the temperature rise during Joule heating, which can generate more intrinsic carriers and lead to thermal runaway in the presence of a constant bias voltage. This article develops a simple model for the thermal runaway effect in doped silicon cantilevers. The model relates the electrical conductivity in the cantilever to the temperature-dependent carrier concentrations in silicon and is consistent with the available experimental data.

This article investigates the thermal runaway effect due to intrinsic carrier generation in micromachined cantilevers made from doped silicon. Each of the micromachined cantilevers incorporates a heating element in the form of a lightly doped, high-resistivity region near the tip. The rest of the cantilever is heavily doped and has low electrical resistance (Figure 1). When electrical current flows through the cantilever, power is dissipated mainly within the high-resistivity heater region, leading to significant heating of the tip.

The heated tip of the cantilever can be used for a variety of tasks such as high-density thermomechanical data storage [1–3]. In one version of this storage method, an atomic force microscope (AFM) cantilever is fabricated with an integrated out-of-plane tip. The tip is put in contact with a rotating polycarbonate disk, and electrical heating pulses applied to the cantilever enable nanoindentations to be formed on the disk surface representing data bits. This storage method is being investigated as a possible means of extending mass storage into the 100-Gbit/in.^{2} regime and beyond [3].

The dynamic thermal behavior of the cantilevers—in particular the thermal time constant—greatly affects the data writing rate achievable with the device. As

Received 25 January 1999; accepted 31 March 1999.

The authors would like to thank J. D. Plummer of Stanford for his insightful comments on the thermal runaway phenomenon. They would also like to thank D. Rugar and B. D. Terris of IBM Almaden Research Center and C. F. Quate and T. D. Stowe of Stanford for their invaluable assistance. This work was supported by NSF CAREER awards for Goodson and Kenny and an IBM Fellowship for Chui.

Address correspondence to B. W. Chui, 944 Cardinal Drive, Sunnyvale, CA 94087.

Microscale Thermophysical Engineering, 3:217–228, 1999
Copyright © 1999 Taylor & Francis
1089-3954/99 $12.00 + .00

NOMENCLATURE

A	cross-sectional area of cantilever leg	P_{seg}	rate of heat generation in a leg segment
E_g	band gap of silicon	q	unit electronic charge
h_{eff}	effective coefficient of heat loss	R_{htr}	electrical resistance of the heater region
I_{lever}	current through the cantilever	R_{lever}	electrical resistance of heater-cantilever
k_B	Boltzmann's constant	R_{seg}	electrical resistance of a leg segment
k_{htr}	thermal conductivity of the heater-region material	T	absolute temperature
k_i	thermal conductivity of segment i	T_{htr}	heater temperature
k_{seg}	thermal conductivity of the leg-segment material	T_i	temperature of segment i
k_{Si}	thermal conductivity of silicon	T_{rm}	room temperature
l_{lever}	length of each cantilever leg	T_{seg}	temperature of a cantilever leg segment
l_{seg}	length of a cantilever segment	V_{kink}	kink voltage
n_i	intrinsic carrier concentration	V_{lever}	voltage across the cantilever
$n_{p\,eff\text{-}htr}$	effective carrier (hole) concentration	μ_p	hole mobility in silicon
P_{htr}	rate of heat generation in the heater region		

previously reported, thermal time constants on the order of 1 μs have been demonstrated with geometrically optimized heaters [4]. Separately, it was also observed that significant non-Ohmic effects occurred in the device that might affect steady-state heater behavior, especially during high-voltage operation. In the present work, we have attempted to model the steady-state behavior of the cantilevers with a thermal-electrical model that is based on the physical characteristics of silicon and is derived as much as possible from fundamental principles and published data. Using the model to relate electrical conductivity to temperature-dependent carrier concentrations in silicon, we were able to simulate thermal runaway in the cantilevers. The simulation results agreed closely with measurements.

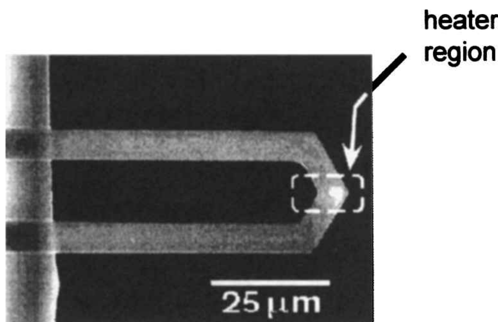

Figure 1. SEM image of a boron-doped heater-cantilever. The region enclosed by the dotted lines represents the lightly doped resistive heater, while the rest of the cantilever is heavily doped. Each cantilever leg is 8 μm wide and 1 μm thick, while the heater region is 8 μm wide.

DEVICE DESCRIPTION

An scanning electron micrograph (SEM) of a sample cantilever is shown in Figure 1. Each cantilever leg is 8 μm wide, as is the heater region at the tip. Actual cantilever lengths range from 50 μm to 250 μm. The thickness is 1 μm. The legs are heavily doped with boron at $5 \times 10^{19}/\text{cm}^3$; the heater region is moderately doped with boron at $8 \times 10^{16}/\text{cm}^3$. The detailed cantilever fabrication process has been described elsewhere [1, 2]. Other types of micromachined heating elements found in the literature include devices made of polysilicon [5, 6] or silicon nitride [7].

MEASUREMENTS AND ANALYSIS

Two sets of electrical I–V measurements were made on the heater-cantilevers: one in vacuum and the other in air. The measurements made in vacuum will be discussed here first. The voltage across a cantilever was swept slowly from 0 to 10 V using a HP4155A semiconductor parametric analyzer, and the measured current was plotted versus voltage. The I–V curve for a 200-μm-long cantilever (Figure 2, series A, solid line) measured in vacuum, for example, shows a decreasing positive slope 0 V to 4.6 V, with a sharp jump in current at a "kink voltage" V_{kink} of 4.6 V. (Similar phenomena were observed for cantilevers of other lengths as well.)

The shape of the curve can be partly explained as follows. The current through the cantilever causes resistive heating, especially in the heater region. The

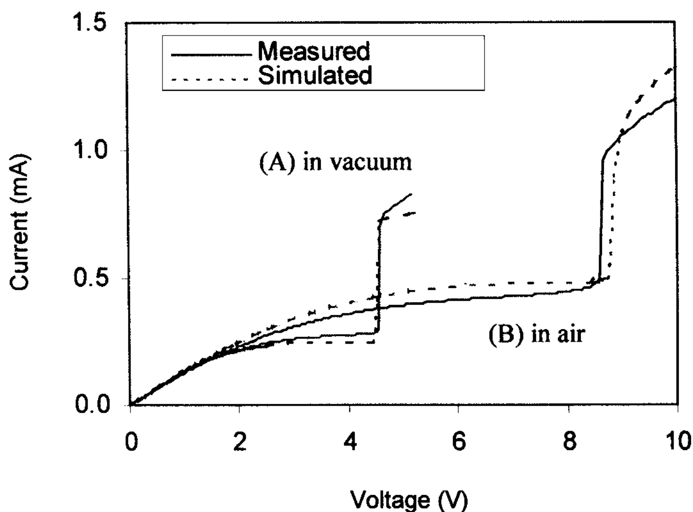

Figure 2. Current versus applied voltage for 200-μm-long electrically heated cantilever (A) in vacuum, (B) in air. The main feature of the curve is the kink at 4.6 V (in vacuum) or 8.8 V (in air), believed to be caused by thermal runaway within the heater region related to intrinsic carrier generation in silicon.

increase in temperature along the cantilever leads to an associated rise in electrical resistance, thereby depressing the I–V curve. This explanation, however, does not account for the kink in Figure 2, where the sharp increase in current implies a sudden decrease in resistance. It is believed that thermal runaway within the heater region might be a factor.

Since the cantilever is made of a semiconductor material, its intrinsic carrier density varies widely with temperature. When the temperature of the heater region reaches a certain level, the intrinsic carrier density in the silicon exceeds the dopant carrier density. Above this temperature, the effective resistance of the heater region is determined largely by the intrinsic carrier density and not the dopant impurity concentration. The extra carriers that become available cause the heater region to decrease in resistance, which in turn allows more current to flow, thereby generating more resistive heating, leading to a further drop in heater resistance. This positive feedback cycle causes the temperature of the heater region to rise suddenly. The temperature continues to increase—and the heater region resistance continues to drop—until the current through the cantilever becomes limited mainly by the leg resistance.

In the following analysis, thermal runaway is assumed to occur only within the heater region, not the cantilever legs. This is because the cantilever legs, being much more heavily doped, are not as susceptible to thermal runaway as the heater region. This means that the intrinsic carrier concentration has a much higher threshold to exceed before it can dominate the leg conductance.

A quantitative device model has been developed to verify the thermal runaway hypothesis. In this model, the cantilever is represented by a series of segments (Figure 3). A set of attributes (resistivity, temperature, thermal conductivity, current, and voltage) is assigned to each segment, and the values of these attributes are solved for using the finite-difference approach in conjunction with the energy balance method. (Other approaches include electrical modeling using SPICE [1, 8, 9].) The attributes are all interdependent, however. For example, resistivity and thermal conductivity depend on temperature, and the current through the cantilever depends on the total resistance of the segments. In this study, simple algebraic formulas are used to represent these dependencies.

The dependence of electrical resistance on temperature is modeled using Eqs. (1)–(3). Note that slightly different equations are used for the legs and the heater region, since the doping levels are different.

The intrinsic carrier concentration n_i in silicon is taken to increase with temperature according to the following pair of equations [10] (see Figure 5, below):

$$n_i = \left[1.5 \times 10^{33} T^3 \exp\left(\frac{-qE_g}{k_B T}\right)\right]^{0.5} \tag{1a}$$

$$E_g = 1.21 - 7.1 \times 10^{-10} n_i^{0.5} T^{-0.5} \tag{1b}$$

where n_i is in units of cm^{-3}, T is the absolute temperature in K, q is the unit electronic charge, k_B is Boltzmann's constant (8.62×10^{-5} eV/K), and E_g is the band gap of silicon in eV. This is an empirical fit to published data [10].

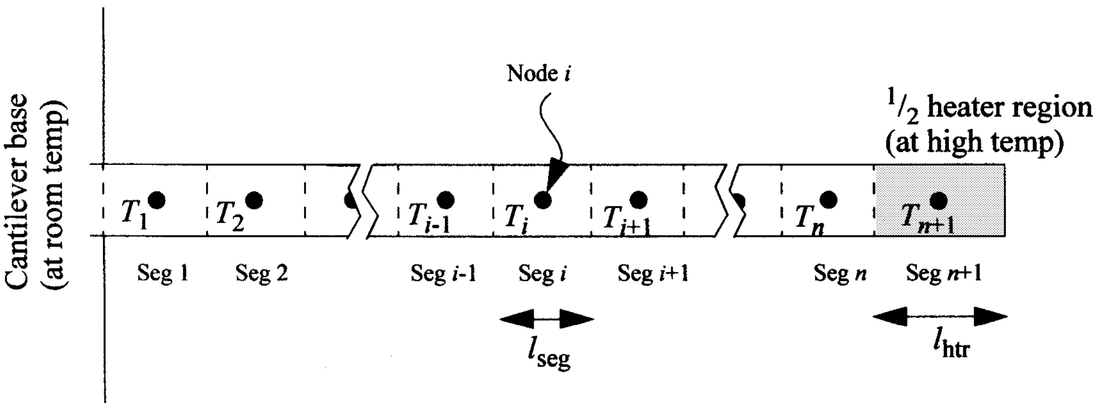

Figure 3. Thermal-electrical model of heater-cantilever. The cantilever is modeled as a series of segments each with its own set of attributes including temperature, thermal conductivity, electrical resistance, and current. A finite-difference equation can be formulated for each segment (and associated node), reflecting the balance of heat flow between itself and neighboring segments as well as electrical heat generation and possible heat loss to the surrounding air. Note that only a half-model (representing only one cantilever leg and half the heater region) is needed because of the symmetrical shape of the cantilever.

The carrier (hole) mobility μ_p in silicon within the heater region is assumed to vary with heater temperature T_{htr} as

$$\mu_p(T_{\mathrm{htr}}) = \mu_p(T_{\mathrm{rm}})\left(\frac{T_{\mathrm{htr}}}{T_{\mathrm{rm}}}\right)^{-1.7} \tag{2a}$$

This approximates a more complicated empirical fit to experimental data [10]. Here, T_{rm} stands for room temperature (300 K). Meanwhile, the corresponding equation for a cantilever leg segment is

$$\mu_{p(T_{\mathrm{seg}})} = \mu_{p(T_{\mathrm{seg}})}\left(\frac{T_{\mathrm{seg}}}{T_{\mathrm{rm}}}\right)^{-0.58} \tag{2b}$$

where T_{seg} is temperature of a particular segment of the cantilever leg in the model.

Note that the absolute value of the exponent in Eq. (2b) is smaller than that in (2a) in order to account for the weaker temperature dependence of hole mobility in heavily doped silicon [11, 12].

As indicated in Eqs. (1) and (2), the electrical resistance of the heater region $R_{\mathrm{htr}}(T_{\mathrm{htr}})$ is assumed to depend only on the effective carrier (hole) concentration $n_{p\mathrm{eff\text{-}htr}}(T_{\mathrm{htr}})$ and carrier (hole) mobility $\mu_{p\text{-}\mathrm{htr}}(T_{\mathrm{htr}})$. In particular, the value of n_p is taken to be equal to the dopant density n_{boron} or the intrinsic carrier density $n_i(T_{\mathrm{htr}})$, whichever is greater at the temperature in question. (This is the crux of the thermal runaway hypothesis.) The heater resistance therefore is given by

$$R_{\mathrm{htr}(T_{\mathrm{htr}})} = R_{\mathrm{htr}(T_{\mathrm{rm}})}\frac{n_{p\,\mathrm{eff\text{-}htr}(T_{\mathrm{rm}})}}{n_{p\,\mathrm{eff\text{-}htr}(T_{\mathrm{htr}})}}\frac{\mu_{p\text{-}\mathrm{htr}}(T_{\mathrm{rm}})}{\mu_{p\text{-}\mathrm{htr}}(T_{\mathrm{htr}})} \tag{3a}$$

It should be reiterated that the value of R_{htr} here corresponds to half the actual heater resistance, since this analysis uses a half-cantilever model.

As for the legs, the electrical resistance of a leg segment $R_{\mathrm{seg}}(T_{\mathrm{seg}})$ is assumed to depend only on its carrier (hole) mobility $\mu_{p\text{-}\mathrm{seg}}(T_{\mathrm{seg}})$:

$$R_{\mathrm{seg}(T_{\mathrm{seg}})} = R_{\mathrm{seg}(T_{\mathrm{rm}})}\frac{\mu_{p\,\mathrm{seg}(T_{\mathrm{rm}})}}{\mu_{p\,\mathrm{seg}(T_{\mathrm{seg}})}} \tag{3b}$$

Data on the temperature dependence of the thermal conductivity of heavily doped silicon [13] are limited. For simplicity, the thermal conductivity of the cantilever material is assumed here to vary inversely as the absolute temperature:

$$k_{\mathrm{htr}(T_{\mathrm{htr}})} = [k_{\mathrm{htr}(T_{\mathrm{rm}})}]^{-1} \tag{4a}$$

$$k_{\mathrm{seg}(T_{\mathrm{seg}})} = [k_{\mathrm{seg}(T_{\mathrm{rm}})}]^{-1} \tag{4b}$$

where k_{htr} and k_{seg} are the thermal conductivities of the heater region material and the cantilever leg segment material, respectively.

Finally, the rate of heat generation in the heater region P_{htr} and each leg segment P_{seg} is given by

$$P_{htr} = [R_{htr}(T_{htr})](I_{lever}^2) \tag{5a}$$

$$P_{seg} = [R_{seg}(T_{seg})](I_{lever}^2) \tag{5b}$$

where I_{lever} is the current flowing through the cantilever. The value of I_{lever} is given by

$$I_{lever} = \frac{V_{lever}/2}{R_{htr(T_{htr})} + \Sigma_{\text{all-segments}} R_{seg(T_{seg})}} \tag{6}$$

Here, V_{lever} is simply the voltage applied across the entire cantilever. The reason for dividing V_{lever} by 2 is that only half the applied voltage appears across the one-legged cantilever model.

Based on Eqs. (1)–(6), a finite-difference equation can be formulated for each node using the energy-balance method. Only conduction through the cantilever material and electrical heat generation within the cantilever is considered. Calculations show that radiation and convection are relatively insignificant sources of heat loss within the temperature range of interest [2].

For node i, the finite-difference equation is

$$(T_i - T_{i-1})\frac{(k_{i,i-1})A}{l_{seg}} = (T_{i+1} - T_i)\frac{(k_{i+1,i})A}{l_{seg}} + (I_{lever})^2 R_{seg} \tag{7}$$

where T_i is the temperature of segment i, $k_{i,i-1}$ is the average thermal conductivity of segments i and $i-1$, A is the cross-sectional area of the cantilever leg, and l_{seg} is the length of a segment.

A system of $n+1$ simultaneous equations can be formulated for the cantilever as a whole, where $n =$ (cantilever length)/(segment length), with the $(n+1)$th segment representing the heater region.

Using an iterative technique, Eqs. (1)–(7) can be solved simultaneously to yield mutually compatible solutions for T_i, T_{htr}, $n_{p\,eff}$, $(R_{seg})_i$, R_{htr}, k_i, and I_{lever} for any given value of V_{lever}. The following parameter values are used (all values are for room temperature, 300 K): resistance of each leg = 1.65 kΩ (i.e., total for two legs is 3.3 kΩ), $l_{seg} = 5\ \mu$m (i.e., there are 40 segments in a 200-μm-long leg, implying $R_{seg} = 412.5\ \Omega$), R_{htr} in the half-cantilever model = 2 kΩ (i.e., 4 kΩ in the actual cantilever), $k_{Si} = 52$ W/m K (for a 1-μm-thick silicon layer doped at $5 \times 10^{19}/\text{cm}^3$).

It should be noted that the thermal conductivity value for silicon used for this analysis (52 W/m K at room temperature) is significantly lower that the standard value of 148 W/m K [14]. Experimental studies [11, 12] have shown that the thermal conductivities of doped silicon samples differ substantially from that of

pure samples. This is because phonons, which dominate heat current in silicon, scatter strongly with impurity atoms and electrons in impure samples [15, 16]. Existing thermal conductivity data suggest that the thermal conductivities of heavily doped silicon samples depend weakly on dopant species and vary with dopant concentration in a matter that can be reasonably well described using a semiempirical thermal conductivity model [13, 17]. The present study uses a thermal conductivity value corrected for the predicted effects of high dopant concentration and 1-μm-scale layer thickness [18, 19] consistent with the cantilever fabrication process [1]. This value has also been tested in previously reported thermal analyses of micromachined heater-cantilevers [1, 2] with favorable results.

The results for I_{lever} versus V_{lever} are plotted in Figure 2 (series A, dotted line). The calculations were performed in MATLAB. Note the close agreement between simulation and experiment. This confirms the validity of the thermal runaway hypothesis, i.e., that thermal generation of intrinsic carriers in the heater is indeed responsible for the sharp jump in the I–V curve.

Figure 4 shows the estimated variation of heater temperature T_{htr} and intrinsic carrier concentration n_i with temperature. Note the sharp jump in both quantities at 4.6 V. This is what causes the sudden increase in current in Figure 2. It is also interesting to note in Figure 5 that the heater region resistance falls drastically at high temperatures with increasing intrinsic carrier generation. In fact, the effect is so pronounced that the heater region resistance eventually becomes negligible compared to the cantilever leg resistance.

Also, note the very high estimated temperature of the heater above 4.6 V in Figure 4. Here, due to the high current, substantial heat generation is occurring not only in the heater region, but in other parts of the cantilever as well. At these temperatures the heater should start to glow. Indeed, this prediction was found to be true, as light emitted from the cantilever was visible to the naked eye during the measurements.

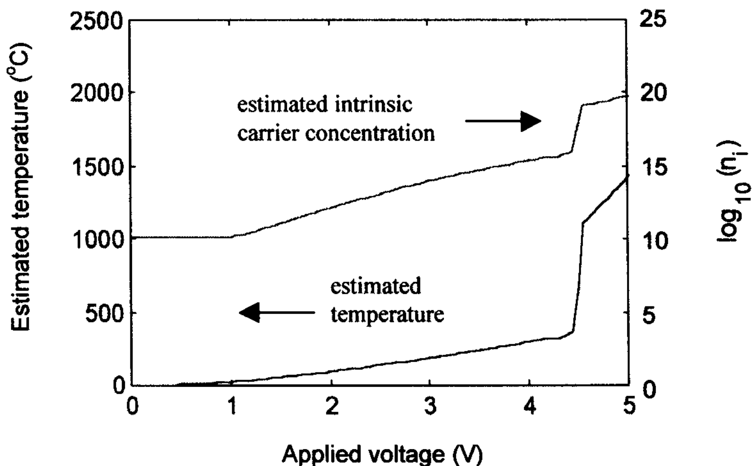

Figure 4. Estimated carrier concentration and heater temperature versus applied voltage.

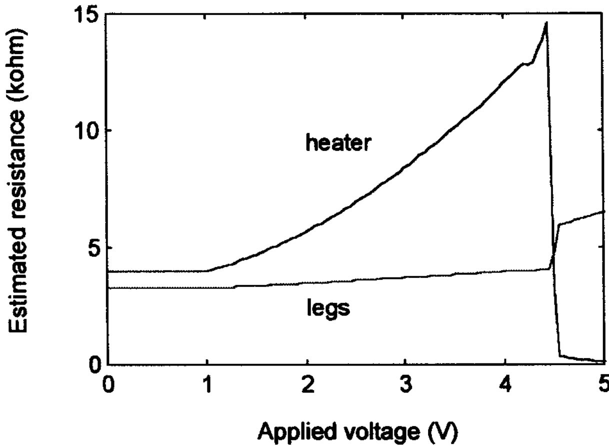

Figure 5. Estimated electrical resistance of cantilever legs and heater region versus applied voltage.

In order to further establish the validity of the thermal-electrical model, Eqs. (1)–(7) were solved for not only for a 200-μm-long cantilever, but also for cantilevers of length 50, 70, 100, 150, and 250 μm. In each case, the number of leg segments in the model was varied to match the specific cantilever length. (Measurements showed that the electrical resistances of the cantilevers could be approximated by the linear equation $R_{\text{lever}} = 4000 + 1.65 \times 10^9\, l_{\text{lever}}$, where R_{lever} is the resistance of the entire heater-cantilever in ohms and l_{lever} is the length of each leg in meters.) For each cantilever length, the value of V_{kink} was calculated. Figure 6 (series A) shows a plot of V_{kink} versus l_{lever}, in which the predicted values are shown compared against experimentally measured data. Close agreement is observed for all cantilever lengths, confirming the validity of the model.

Finally, the entire experiment was repeated with the measurements being performed in air instead of vacuum. In order to take into account an additional heat loss mechanism—that of conduction through the air—an effective coefficient of heat loss h_{eff} was defined. This parameter represents the effectiveness of air cooling per unit length of the cantilever, and has units W/m K. The nodal energy-balance equation then becomes

$$(T_i - T_{i-1})\frac{(k_{i,i-1})A}{l_{\text{seg}}} + h_{\text{eff}} l_{\text{seg}}(T_i - T_{\text{rm}}) = (T_{i+1} - T_i)\frac{(k_{i+1,i})A}{l_{\text{seg}}} + (I_{\text{lever}})^2 R_{\text{seg}} \tag{8}$$

where T_{rm} is room temperature (300 K). Here, h_{eff} is taken to be 0.1 W/m K. Values of I_{lever} versus V_{lever} were calculated as before using the thermal-electrical model for each cantilever length. See Figure 2 (series B) for the 200-μm cantilever

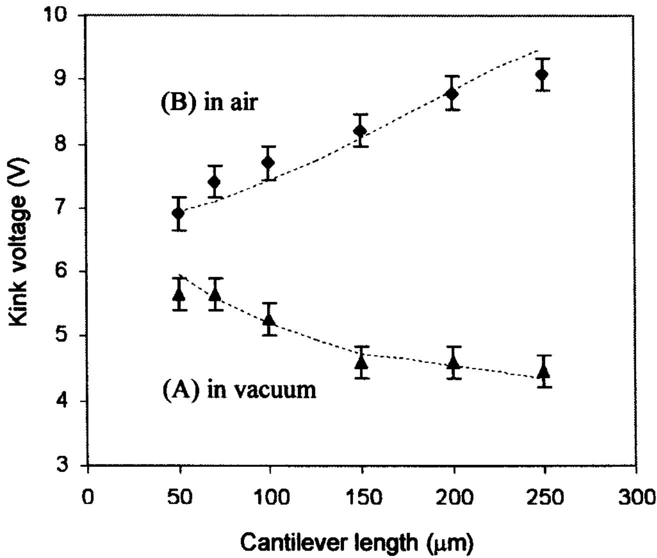

Figure 6. Kink voltage versus cantilever length, for cantilever heating measurements performed in vacuum (series A) and in air (series B). The dotted lines represent predictions based on the thermal-electrical model.

case, in which the simulated curve and the measured data again show a high degree of correlation, just as they did for the vacuum measurements. In addition, predicted values of V_{kink} in air for various cantilever lengths were compared with the measured data, and the results in this case (Figure 6, series B) also agree.

SUMMARY

Micromachined cantilevers with resistive heating filaments were fabricated to investigate semiconductor thermal runaway due to intrinsic carrier generation. Steady-state measurements of the I–V characteristics of the heater-cantilever gave a curve showing a sharp jump in current at a characteristic voltage. A thermal-electrical model was formulated to explain the phenomenon. Simple formulas were used to relate silicon material properties such as electrical resistance and thermal conductivity to temperature. In particular, the model embodies the hypothesis that at high temperatures, the intrinsic carrier concentration in the heater region of the cantilever increases to such an extent that it exceeds the external dopant concentration, leading to a marked decrease in electrical resistance. This results in a positive-feedback cycle that produces higher current, stronger heating, and still higher temperatures. The cycle is stopped only when the cantilever leg resistance starts to dominate and limit current flow.

Values of kink voltage predicted for various cantilever lengths using the model were compared against measured values, and a high degree of correlation was observed. The model was accurate for vacuum and air environments.

REFERENCES

1. B. W. Chui, T. D. Stowe, Y. S. Ju, K. E. Goodson, T. W. Kenny, H. J. Mamin, B. D. Terris, R. P. Ried, and D. Rugar, Low-Stiffness Silicon Cantilevers with Integrated Heaters and Piezoresistive Sensors for High-Density AFM Thermomechanical Data Storage, *J. Microelectromech. Syst.*, vol. 7, no. 1, pp. 69–78, 1998.
2. B. W. Chui, Advanced Silicon Micromachined Cantilevers for Atomic Force Microscope Data Storage, Ph.D. thesis, Stanford University, Stanford, CA, 1998. *See also* B. W. Chui, *Microcantilevers for Atomic Force Microscope Data Storage*, Kluwer, Boston, 1999.
3. G. Binnig, M. Despont, U. Drechsler, W. Haberle, M. Lutwyche, P. Vettiger, H. J. Mamin, B. W. Chui and T. W. Kenny, Ultra High-Density AFM Data Storage with Erase Capability, *Appl. Phys. Lett.*, vol. 74, no. 9, pp. 1329–1331, 1999.
4. B. W. Chui, H. J. Mamin, B. D. Terris, D. Rugar, K. E. Goodson, and T. W. Kenny, Micromachined Heaters with 1-μs Thermal Time Constants for AFM Thermomechanical Data Storage, *Proc. Transducers '97, Int. Conf. on Solid-State Sensors and Actuators*, Chicago, IEEE cat. no. 97CH8267, pp. 1085–1088, 1997.
5. H. J. Comtois and V. M. Bright, Surface Micromachined Polysilicon Thermal Actuator Arrays and Applications, *Proc. Solid-State Sensor and Actuator Workshop*, Hilton Head, SC, pp. 174–177, 1996.
6. E. H. Yang and H. Fujita, Fabrication and Characterization of U-Shaped Beams for the Determination of Young's Modulus Modification Due to Joule Heating of Polysilicon Microstructures, *Proc. Transducers '97, Int. Conf. on Solid-State Sensors and Actuators*, IEEE cat. no. 97CH8267, pp. 603–606, 1997.
7. J. H. Das, N. C. MacDonald, Micromachined Field Emission Cathode with an Integrated Heater, *J. Vac. Sci. Technol. B*, vol. 13, no. 6, pp. 2432–2435, 1995.
8. B. W. Chui, H. J. Mamin, B. D. Terris, D. Rugar, K. E. Goodson, and T. W. Kenny, Micromachined Heaters with 1-microsecond Thermal Time Constants for AFM Thermomechanical Data Storage, *Proc. Transducers '97, Int. Conf. on Solid-State Sensors and Actuators*, Chicago, IEEE cat. no. 97CH8267, pp. 1085–1088, 1997.
9. J. T. Butler, V. M. Bright, and W. D. Cowan, SPICE Modeling of Polysilicon Thermal Actuators, *Proc. SPIE*, vol. 3224, pp. 284–293, 1997.
10. R. S. Muller and T. I. Kamins, *Device Electronics for Integrated Circuits*, 2d ed., Wiley, New York, 1977.
11. G. A. Slack, Thermal Conductivity of Pure and Impure Silicon, Silicon Carbide, and Diamond, *J. Appl. Phys.*, vol. 35, pp. 3460–3466, 1964.
12. L. Weber and E. Gmelin, Transport Properties of Silicon, *Appl. Phys. A*, vol. 53, no. 2, pp. 136–140, 1991.
13. Y. S. Ju and K. E. Goodson, Phonon Scattering in Silicon Films with Thickness of Order 100 nm, *Appl. Phys. Lett.*, vol. 74, no. 20, pp. 3005–3007, 1999.
14. F. P. Incropera and D. P. de Witt, *Fundamentals of Heat and Mass Transfer*, 3d ed., Wiley, New York, 1990.
15. S. Tamura, Isotope Scattering of Dispersive Phonons in Ge, *Phys. Rev. B*, vol. 27, pp. 858–866, 1983.
16. E. F. Steigmeir, Thermal Conductivity of Semi-conducting Materials, in R. P. Tye (ed.), *Thermal Conductivity*, Academic Press, New York, 1969.

17. Y. S. Ju and K. E. Goodson, Heat Transport in Silicon Nanostructures, to be presented at ASME Natl. Heat Transfer Conf., 1999.
18. M. Asheghi, M. N. Touzelbaev, Y. K. Leung, S. S. Wong and K. E. Goodson, Temperature-Dependent Thermal Conductivity of Single-Crystal Silicon Layers in SOI Substrates, *Trans. ASME*, vol. 120, pp. 30–36, 1998.
19. M. Asheghi, K. Kurabayashi, R. Kasnavi, J. D. Plummer, and K. E. Goodson, Thermal Conduction in Doped Single-Crystal Silicon Films, to be presented at National Heat Transfer Conf., Sept. 1999.